Supporting Information

Twinned Crystal $Cd_{0.9}Zn_{0.1}S/MoO_3$ Nanorods S-Scheme Heterojunctions as Promising Photocatalysts for Efficient Hydrogen Evolution

Jie Chen [a], Ying Xie [a,*], Haitao Yu [a], Zhenzi Li [b], Wei Zhou[*, b]

[a] Key Laboratory of Functional Inorganic Material Chemistry, Ministry of Education, School of Chemistry and Materials Science, Heilongjiang University, Harbin, 150080, PR China.

[b] Shandong Provincial Key Laboratory of Molecular Engineering, School of Chemistry and Chemical Engineering, Qilu University of Technology (Shandong Academy of Sciences), Jinan, Shandong 250353, PR China.

*Corresponding author: Ying Xie

E-mail: xieying@hlju.edu.cn (Dr. Ying Xie).

*Corresponding author: Wei Zhou

E-mail: wzhou@qlu.edu.cn

1. Experimental

1.1. Material preparation

The chemical reagents used were ammonium molybdate ($(NH_4)_2MoO_4 \cdot 10H_2O$, Aladdin Reagent Co.), nitric acid (HNO_3, Aladdin Reagent Co.), cadmium acetate dihydrate ($Cd(CH_3COO)_2 \cdot 2H_2O$, Bide Pharmaceuticals), zinc acetate dihydrate ($Zn(CH_3COO)_2 \cdot 2H_2O$, Guangfu Group), thioacetamide (C_2H_5NS Aladdin Reagent Co.), and ethylenediamine, and they were all analytical grade and used without further purification.

MoO_3 was synthesized by a hydrothermal reaction. In the synthesis, 1.0 g of ammonium molybdate was first dispersed into a solution of concentrated nitric acid and deionized water at a ratio of 1:5 to form a mixed solution. After stirring for about 30 min, the above solution was transferred to a 100 mL polyethylene lined stainless steel autoclave and kept at 180 ℃ for 24 h. After the reaction was completed, the mixture was cooled to room temperature. After centrifugation and washing three times with deionized water and ethanol, the product was dried in a vacuum oven at 60 °C for 12 h to obtain MoO_3.

$Cd_{0.9}Zn_{0.1}S$ was synthesized via ethylenediamine as an auxiliary pathway via a hydrothermal reaction.[1] 18 mmol $Cd(CH_3COO)_2 \cdot 2H_2O$ and 2 mmol $Zn(CH_3COO)_2 \cdot 2H_2O$ was added into 50 mL deionized water under constant stirring. 25 mmol thioacetamide and 10 mL ethylenediamine were then added to the above aqueous solution, and the mixture was stirred for 1 h. Then, the above solution was transferred to a 100 mL polyethylene lined stainless steel autoclave and kept at 180 °C for 12 h. After the reaction was completed, the mixture was cooled to room temperature. After centrifugation and washing three times with deionized water and ethanol, the product was dried in a vacuum oven at 60 °C for 12 h to obtain $Cd_{0.9}Zn_{0.1}S$.

$Cd_{0.9}Zn_{0.1}S/MoO_3$ was prepared by in situ growth. In the synthesis process, the prepared MoO_3 was firstly dispersed in 30 mL of ethanol and ultrasonicated for 3 h, and $Cd_{0.9}Zn_{0.1}S$ was dispersed in 5 mL of ethanol and similarly ultrasonicated for 3 h. Then MoO_3 and $Cd_{0.9}Zn_{0.1}S$ were mixed and stirred for 40 min, and the above solution was transferred to a 100 mL polyethylene lined stainless steel autoclave and kept at 180 °C for 24 h. After the reaction was completed, the mixture was cooled to room temperature. After centrifugation and washing three times with deionized water and ethanol, the product was dried in a vacuum oven at 60 °C for 12 h. Finally, $Cd_{0.9}Zn_{0.1}S/MoO_3$ was obtained. According to the addition of different amounts of $Cd_{0.9}Zn_{0.1}S$, two proportional composites were synthesized. 0.03% $Cd_{0.9}Zn_{0.1}S/MoO_3$, 0.09% $Cd_{0.9}Zn_{0.1}S/MoO_3$, respectively.

1.2 Characterizations

X-ray diffraction (XRD) patterns were obtained by a Bruker D8 diffractometer using Cu Kα radiation. The microstructures were identified by scanning an electron microscopy (SEM, FEI Sirion 200) and a transmission electron microscopy (JEM-2100F). Nitrogen adsorption-desorption isotherms, specific surface areas, and pore size distributions were collected on an ASAP 2460 aperture analyzer. Optical absorption and diffuse reflectance spectrometry (UV-DRS) were performed using the UV-Vis spectrophotometer (Lambda 950). X-band electron paramagnetic resonance (EPR) spectra were recorded using a BRUKER N500 EPR spectrometer. The photo-luminescence (PL) were detected on a fluorescence spectrometer (PerkinElmer FL 6500) with an excitation wavelength of 247 nm. X-ray photoelectron spectroscopy (XPS) was used to clarify the elemental chemical

composition of different samples by Japan Shimadzu/Kratos Axis Supra systems. Raman spectroscopy was used to analyze lattice vibration of the samples by the HORIBA HR 800 spectrometer. Fourier-transform infrared spectroscopy (FT-IR) was recorded on a Perkin-Elmer Spectrum One spectrometer using KBr pellets.

1.3 Photocatalyst test

The photocatalytic hydrogen production experiments were performed in a photocatalytic hydrogen production system (Labsolar-6A, Beijing Perfect Light Technology Co., Ltd.). A cut-off filter (λ > 400 nm) was used to remove the UV light to produce visible light, and a 300 W Xe-lamp was used as the light source. In a typical photocatalytic test, 50 mg of photocatalyst was dispersed in 100 mL of an aqueous solution containing 10 ml of lactic acid and 90 ml of water as the sacrificial reagent, and the solution was stirred continuously during the test. Then, an appropriate amount of H_2PtCl_6 was added and reduced via the photo-deposition method to load 1% Pt on the surface of the photocatalyst as co-catalysts. Before visible light irradiation, the opening was sealed with a quartz cap with a silicone rubber gasket, and the test apparatus was evacuated for 30 min to remove O_2 from the reaction system. Finally, the mixture was exposed under radiation and the gas product was analyzed using a gas chromatograph (Techcomp 7900, TCD, Ar carrier) to determine hydrogen production.

1.4 Photoelectrochemical measurements

The samples were tested on a Princeton Versa STAT 2 electrochemical workstation with a standard three-electrode system (Ag/AgCl as reference electrode and Pt foil as counter electrode) and the electrolyte was a 0.2 M Na_2SO_4 solution. First, 50 mg sample was dispersed into ethanol with ultrasonic treatment for 4 h. After the ultrasonic cleaning of FTO in ethanol, the dispersion was then evenly sprayed on a FTO glass with an airbrush, and the actual effective surface area is 1.0 cm^2. Finally, the FTO glass was placed in a tube furnace and calcined at 350 °C under a N_2 gas atmosphere with a heating rate of 5 °C/min for 2 h. The FTO glass was cooled down to room temperature. The electrolyte was degassed by purging the solution with N_2 gas for 30 min before the photoelectrochemical test, which was performed using a 300 W Xe-lamp (light intensity of 64.2×10^{-3} w·cm^{-2}) with a pass filter (AM 1.5) as the light source. The carrier density (N_d) can be calculated by the following equation,

$$\mathrm{N}_d = \frac{2}{q\varepsilon\varepsilon_0}[d(1/c^2)/dv]^{-1} \quad (1)$$

where q, ε, ε_0, and c are the change of an electron (1.60×10^{-19} C), the dielectric constant of a semiconductor, the vacuum permittivity (8.854×10^{-12} F·cm^{-1}), and the capacitance of the depletion region, while V and $d(1/c^2)/dv$ are the applied voltage and the slope of a Mott-Schottky plot. Moreover, during the test, a standard three-electrode system was used, with the photocatalyst as the working electrode, Ag/AgCl as the reference electrode, and Pt as the counter electrode. The conversion between the reversible hydrogen electrode (RHE), standard hydrogen electrode (SHE) and normal hydrogen electrode (NHE) is based on the following equations. The conversion between the three-electrode system and the normal hydrogen electrode (NHE) is used in this paper.

$$E(RHE)=E(NHE)+0.0591\times PH \quad (2)$$

$$E(RHE)=E(SHE)+0.0591\times PH+0.2415 \quad (3)$$

E(NHE)=E(Ag/AgCl)+0.197 (4)

The value to correlate the flat band potential and the conduction band is 0.197 V. Furthermore, Scanning Kelvin probe (SKP) measurements (SKP5050 system, Scotland) performed at normal laboratory conditions. The work function(W_F) can be calculated according to equation,

$$W_F(eV) = 5.1 + \frac{\Delta CPD}{1000} \quad (5)$$

Where ΔCPD is the contact potential difference.

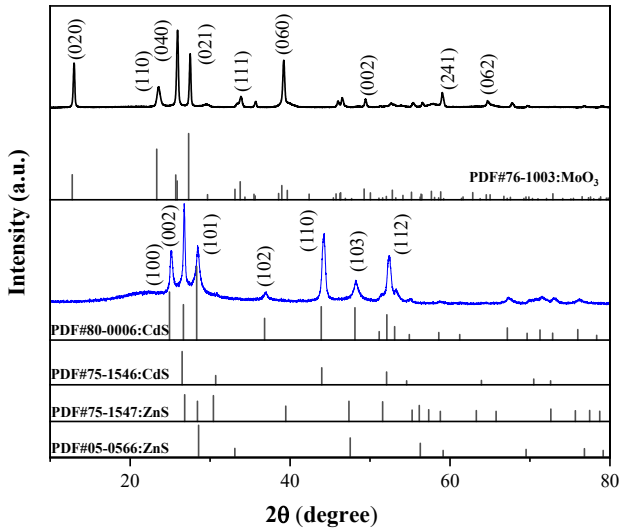

Figure S1. XRD patterns of MoO_3 and $Cd_{0.9}Zn_{0.1}S$.

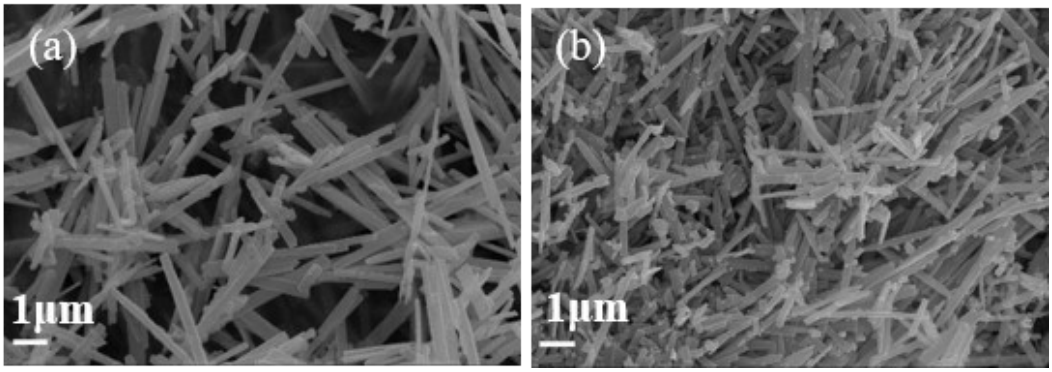

Figure S2. SEM images of (a) MoO_3 and (b) 0.09% $Cd_{0.9}Zn_{0.1}S/MoO_3$.

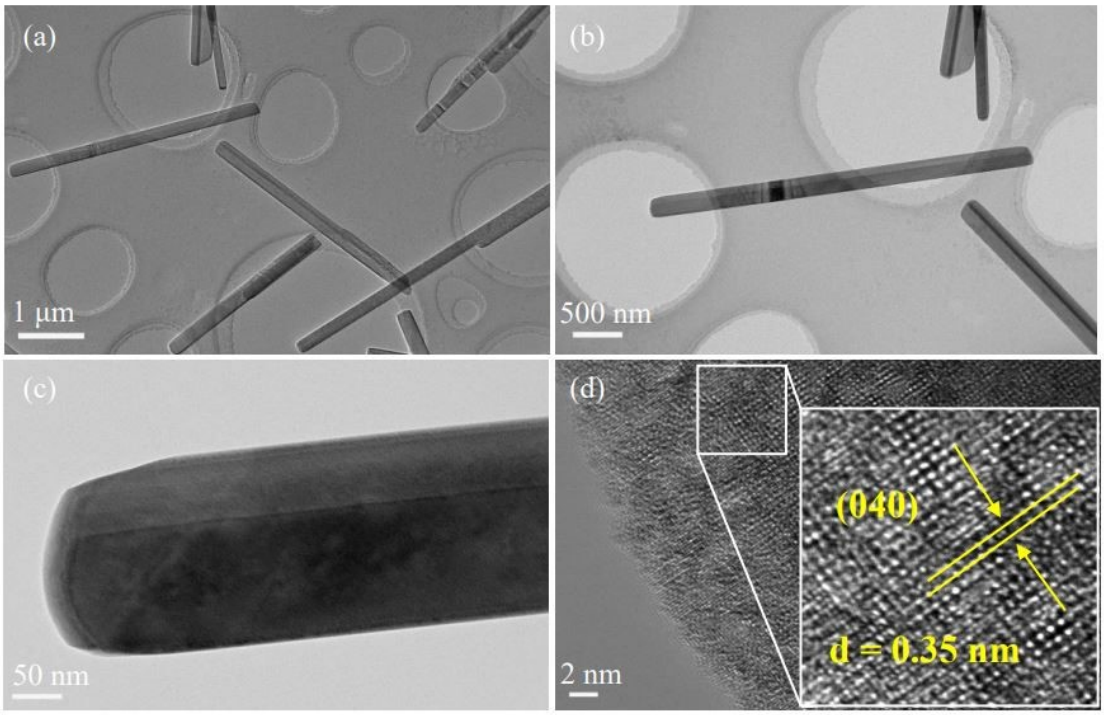

Figure S3. TEM (a, b, c) and HRTEM (b) images of MoO_3.

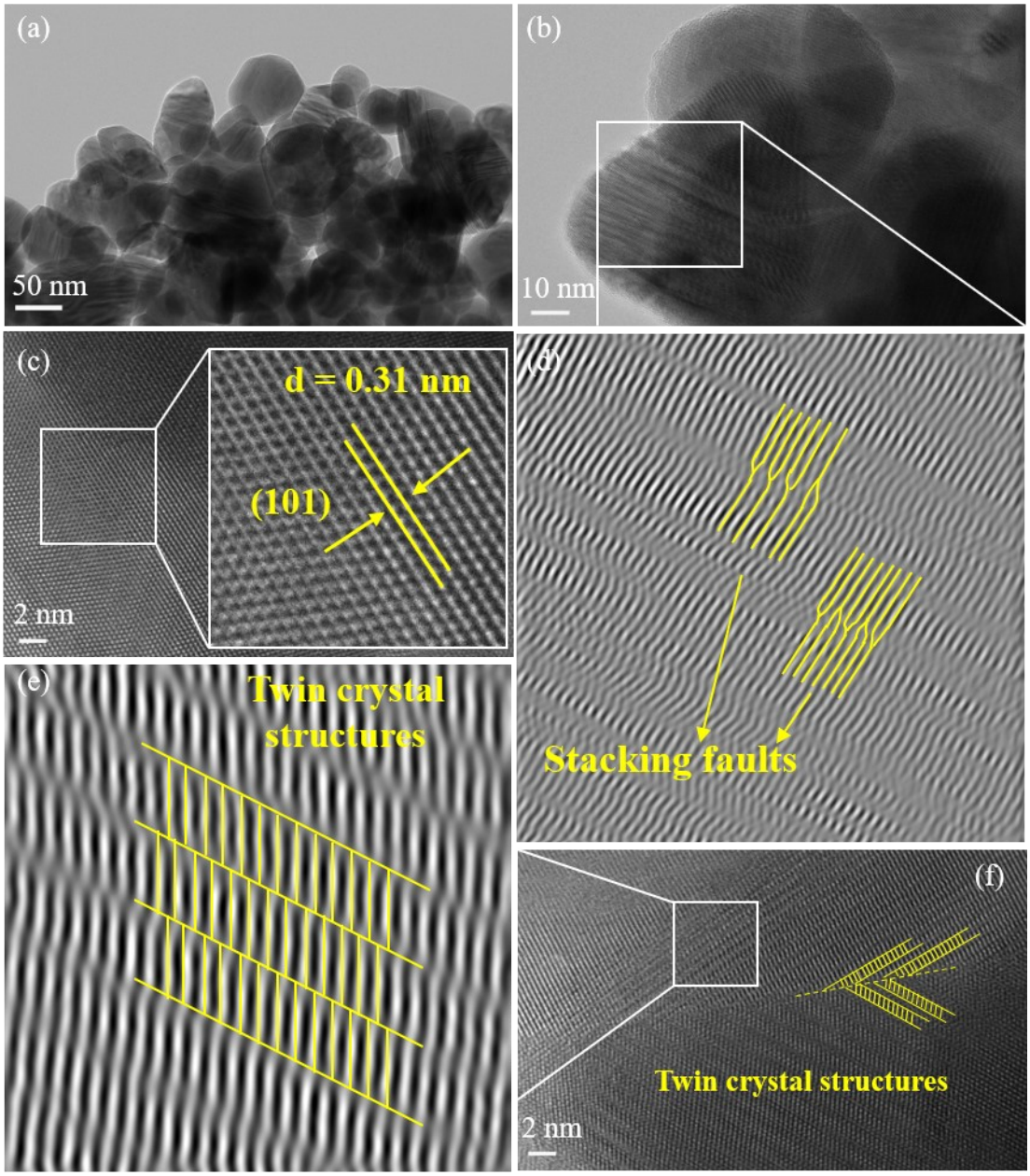

Figure S4. (a, b) TEM, (c) HRTEM images of $Cd_{0.9}Zn_{0.1}S$, and (d, e, f) $Cd_{0.9}Zn_{0.1}S$ twin crystal structure.

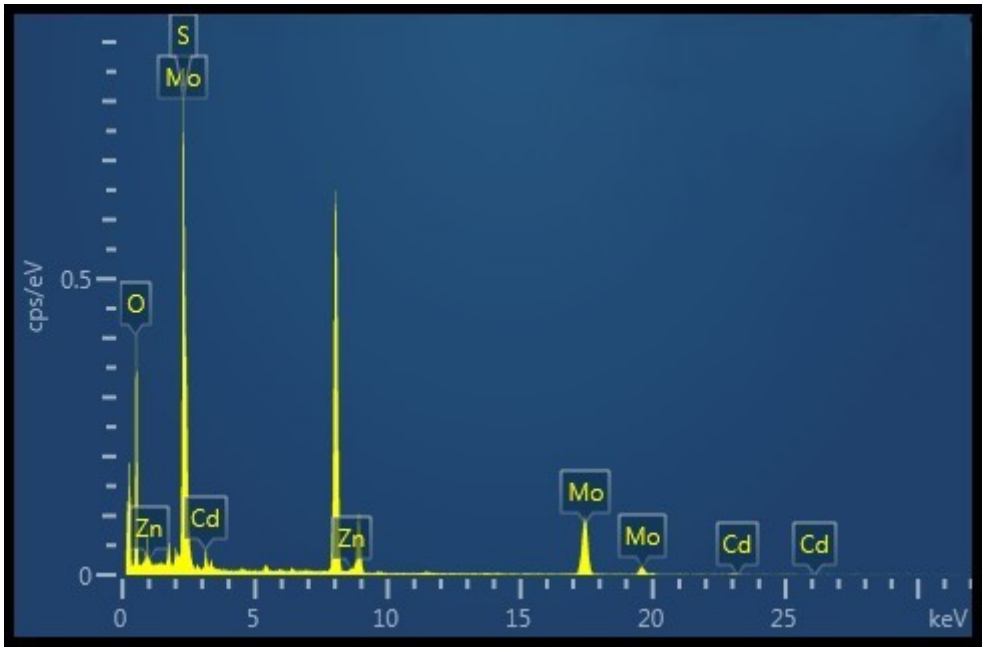

Figure S5. Energy dispersive spectroscopy spectra of 0.09% $Cd_{0.9}Zn_{0.1}S/MoO_3$, respectively.

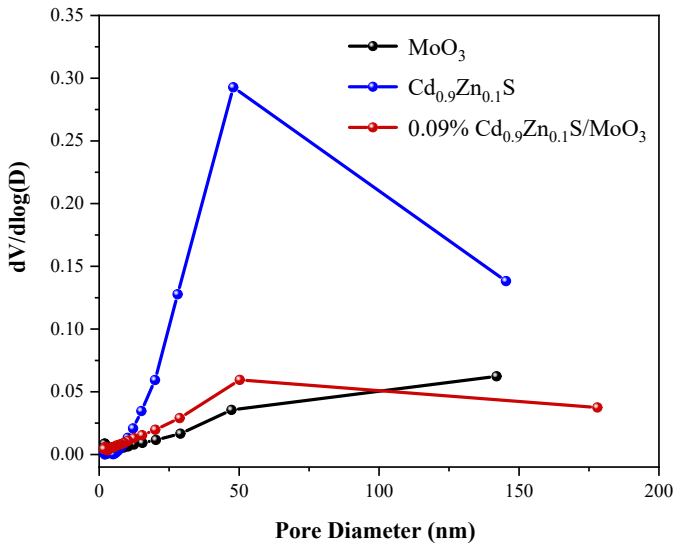

Figure S6. Corresponding pore-size distributions of MoO_3, $Cd_{0.9}Zn_{0.1}S$ and 0.09% $Cd_{0.9}Zn_{0.1}S/MoO_3$, respectively.

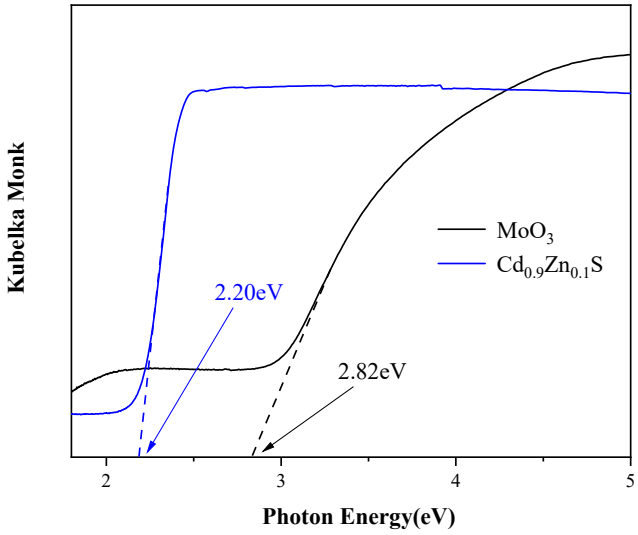

Figure S7. Optical band gaps of MoO_3 and $Cd_{0.9}Zn_{0.1}S$.

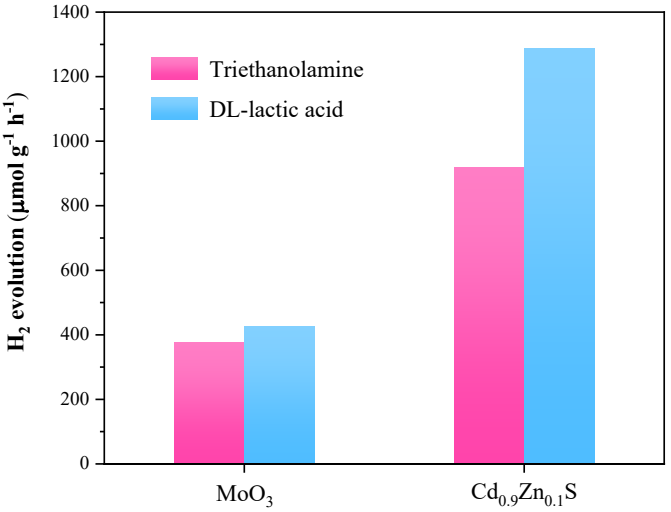

Figure S8. Photocatalytic hydrogen evolution rates of MoO_3, $Cd_{0.9}Zn_{0.1}S$ under triethanolamine and lactic acid.

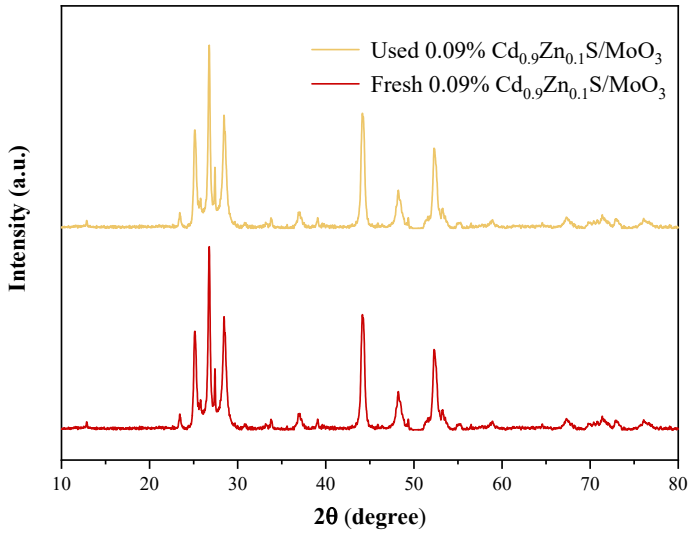

Figure S9. XRD patterns for the fresh and used 0.09% $Cd_{0.9}Zn_{0.1}S/MoO_3$ after 3 cycles.

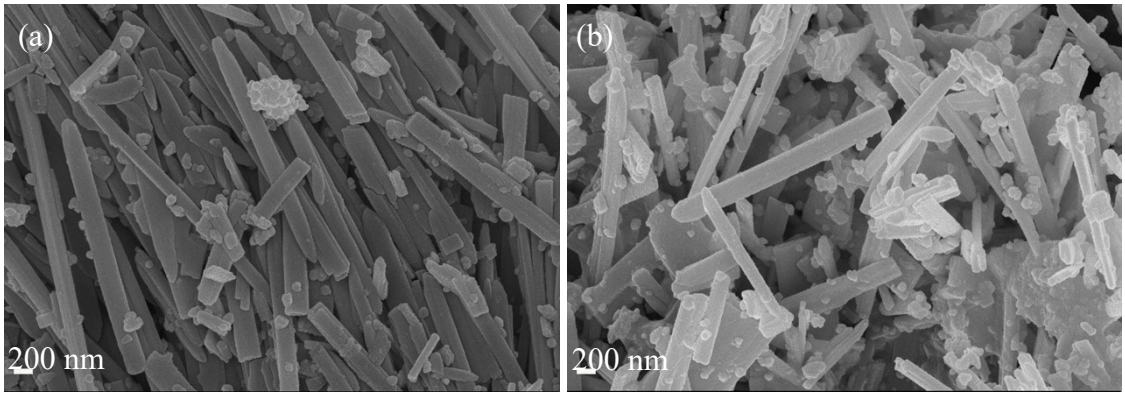

Figure S10. SEM images for the fresh and used 0.09% $Cd_{0.9}Zn_{0.1}S/MoO_3$ after 3 cycles.

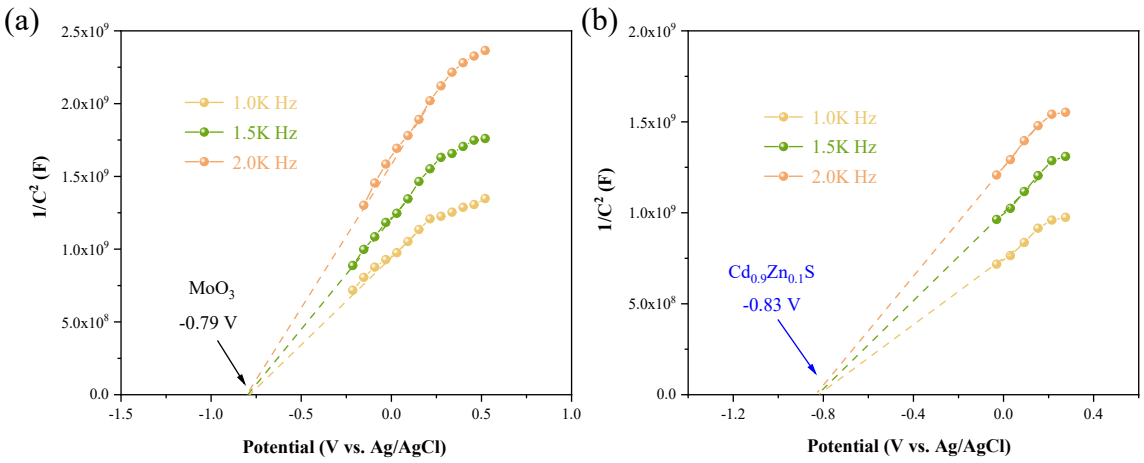

Figure S11. Mott-Schottky plots of MoO_3 and $Cd_{0.9}Zn_{0.1}S$, respectively.

.

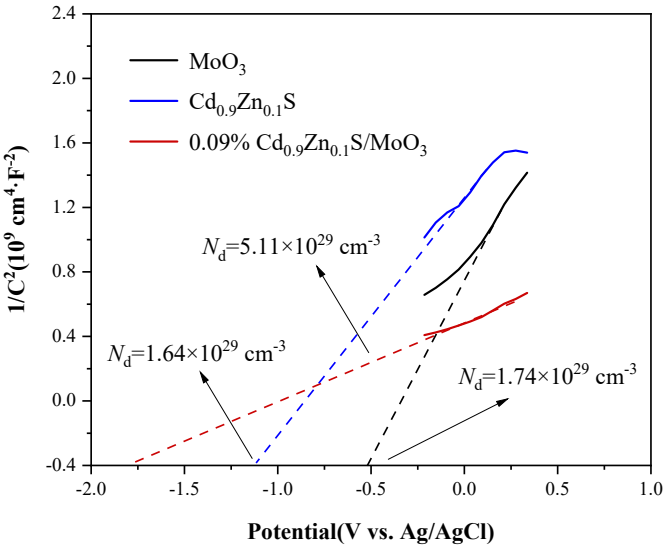

Figure S12. Carrier density plots of MoO_3, $Cd_{0.9}Zn_{0.1}S$ and 0.09% $Cd_{0.9}Zn_{0.1}S/MoO_3$.

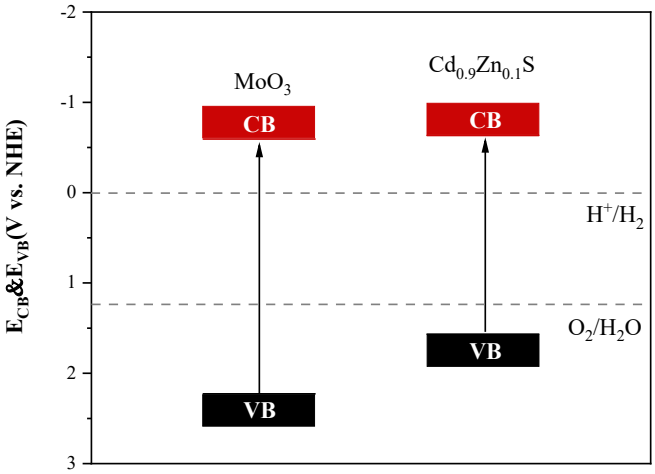

Figure S13. Band structure diagrams for MoO_3 and $Cd_{0.9}Zn_{0.1}S$.

Table S1 BET specific surface areas, pore volumes and pore sizes of different samples.

Samples	S_{BET} (m^2 g^{-1})	Pore volume (cm^3 g^{-1})	Pore size (nm)
MoO_3	8.4423	0.042362	22.6469
$Cd_{0.9}Zn_{0.1}S$	20.4079	0.215579	40.9524
$Cd_{0.9}Zn_{0.1}S/MoO_3$	11.5497	0.062730	24.7506

Table S2 Comparison of photocatalytic H_2 evolution rate of the metal sulfide photocatalysts

Photocatalyst	Sacrificial agent	Light source	H_2 evolution rate ($\mu mol\ h^{-1}\ g^{-1}$)	Ref.
CdS/MnO_x-$BiVO_4$	100 mL solution	300 W Xe ($\lambda>350$ nm)	1010	2
CuO/CdS/$CoWO_4$	Na_2S/Na_2SO_3	300 W Xe ($\lambda>420$ nm)	457.9	3
CdS/graphene	Lactic acid	350 W Xe ($\lambda>420$ nm)	1120	4
g-C_3N_4-AQ-MoO_3	TEOA	300 W Xe (A.M.1.5)	673	5
1.5wt% Pt MoO_3/g-C_3N_4	TEOA	300 W Xe ($\lambda>400$ nm)	205.2	6
CdS/MoO_3	0.25 M Na_2S/0.25 M Na_2SO_3	300 W Xe ($\lambda>420$ nm)	201.4	7
Amine-CdS/MoO_3	0.25 M Na_2S/0.25 M Na_2SO_3	300 W Xe ($\lambda>420$ nm)	1029.8	7
Cu_2S/MoO_3	Na_2S/Na_2SO_3	Xe lamp (400 W)	21.568	8
CdZnS	Lactic acid	LDE lamp	449.4	9
rGO/$Cd_xZn_{1-x}S$	0.35 M Na_2S/0.25 M Na_2SO_3	150 W Xe arc lamp	1060	10
$Cd_{0.5}Zn_{0.5}S$	0.35 M Na_2S/0.25 M Na_2SO_3	300 W Xe ($\lambda>400$ nm)	1023	11
$In_2O_3/Cd_{0.5}Zn_{0.5}S$	0.35 M Na_2S/0.25 M Na_2SO_3	300 W Xe ($\lambda>420$ nm)	1110	12
ZnS	0.35 M Na_2S/0.25 M Na_2SO_3	300 W Xe ($\lambda>420$ nm)	83.77	13
W-ZnS	0.35 M Na_2S/0.25 M Na_2SO_3	300 W Xe ($\lambda>400$ nm)	63.68	14
0.09% $Cd_{0.9}Zn_{0.1}S/MoO_3$	**Lactic acid**	**300 W Xe ($\lambda>400$ nm)**	**3909.79**	**This work**

References

1. M. Liu, D. Jing, Z. Zhou and L. Guo, *Nat. Commun.*, 2013, **4**, 2278.
2. D. Gogoi, A. K. Shah, P. Rambabu, M. Qureshi, A. K. Golder and N. R. Peela, *ACS Appl. Mater. Interfaces*, 2021, **13**, 45119-46212.
3. N. Güy, K. Atacan and M. Ozacar, *Renewable Energy*, 2022, **195**, 107-120.
4. Q. Li, B. Guo, J. Yu, J. Ran, B. Zhang, H. Yan and J. R. Gong, *J. Am. Chem. Soc.*, 2011, **133**, 10878-10884.
5. X. Ma, G. Wang, L. Qin, J. Liu, B. Li, Y. Hu and H. Cheng, *Appl. Catal., B*, 2021, **288**, 120025.
6. K. Li, W. Wu, Y. Jiang, Z. Wang, X. Liu, J. Li, D. Xia, X. Xu, J. Fan and K. Lin, *Inorganic Chemistry Frontiers*, 2021, **8**, 1154.
7. S. Wang, X. Zhao, H. M. A. Sharif, Z. Chen, Y. Chen, B. Zhou, K. Xiao, B. Yang and Q. Duan, *Chem. Eng. J.*, 2021, **406**, 126849.
8. S. B. Patil, B. Kishore, K. Manjunath, V. Reddy and G. Nagaraju, *Int. J. Hydrogen Energy*, 2018 **43**, 4003-4014.
9. L. M. Song, S. J. Zhang, D. Liu, S. Sun and J. Wei, *Int. J. Hydrogen Energy*, 2020, **45**, 8234-8242.
10. Q. Li, H. Meng, J. Yu, W. Xiao, Y. Zheng and J. Wang, *Chem. Eur. J*, 2014.
11. L. H. Zhang, F. D. Zhang, H. Xue, J. Gao, Y. Peng, W. Song and L. Ge, *Chin. J. Catal.*, 2021, **42**, 1677-1688.
12. H. Yang, J. Tang, Y. Luo, X. Zhan, Z. Liang, L. Jiang, H. Hou and W. Yang, *Small*, 2021, **17**, 2102307.
13. X. Hao, Y. Wang, J. Zhou, Z. Cui, Y. Wang and Z. Zou, *Appl. Catal., B*, 2018, **221**, 302-311.
14. B. Xiao, T. Lv, J. Zhao, Q. Rong, H. Zhang, H. Wei, J. He, J. Zhang, Y. Zhang, Y. Peng and Q. Liu, *ACS Catal.*, 2021, **11**, 13255-13265.